

# The dynamics of a qubit in a spin-boson environment: a comparison between analytical and numerical method

Peihao Huang<sup>1,2,\*</sup>, Hang Zheng<sup>1</sup>, and Keiichiro Nasu<sup>2</sup>

<sup>1</sup>*Department of Physics, Shanghai Jiao Tong University, Shanghai 200240, P.R.China*

<sup>2</sup>*Solid State Theory Division, Institute of Materials Structure Science, High Energy Accelerator Research Organization (KEK), Tsukuba, Ibaraki 305-0801, Japan*

(Dated: November 12, 2010)

## Abstract

The dynamics of a qubit under the decoherence of a two level fluctuator (TLF) in addition to its coupling to a bosonic bath is investigated theoretically. Two different methods are applied and compared for this problem. One is a perturbation method based on a unitary transformation. With the merit of our unitary transformation, non-adiabatic effect can be taken into account efficiently. And the other one is the numerically exact method, namely the quasi-adiabatic path-integral (QUAPI) propagator technique. We find that the analytical method works well for a wide parameter range and show good agreement with QUAPI. On the other hand, The enhancement and the reduction of quantum decoherence of the qubit is checked with varying bath temperature  $T$  and TLF-bath coupling.

PACS numbers: 03.65.Yz, 03.67.Pp, 03.67.Lx, 05.30.-d

Keywords: Decoherence, open systems, quantum statistical methods

---

\*Electronic address: phhuang@sjtu.edu.cn

## I. INTRODUCTION

Dissipative quantum dynamics is one of the central paradigm in the theoretical physics because of its relation to the various physical and chemical phenomena from the spontaneous emission to electron transfer in molecular, from qubit decoherence to photon harvest in photosynthesis [1–5]. In the last decades, spin-boson model, the simplest possible model to describe dissipation, is studied intensively and offers a comprehensive understanding of the decoherence phenomenon.

In this paper, a variant of the spin-boson model is studied, the overall spin-boson model act as an environment of another spin. This model describes a qubit in dissipative two-level fluctuators (TLF) which is believed to be relevant to the prevailing  $1/f$  noise in the Josephson qubits[6–13]. Only a single spin-boson environment is considered since the qubit dynamics is usually dominated by a particular TLF near resonance with the qubit. An accurate evaluation of this problem is challenging. By employing the flow equation method, Gassmann et.al. studied the spectrum of the correlation functions of this model. And it is studied a lot recently with various perturbation approaches [12–18].

In this paper we examine the effect of the bath temperature and system bath coupling on the qubit dynamics. One commonly believed concept is that temperature and the coupling to noisy bath only play a negative role in preserving the qubit coherence. However, it is pointed out in Ref. [19] that the temperature can help the coherence when the qubit is coupled to a TLF (or spin-boson) environment. To examine this effect we treat the model more rigorously by consider spin-spin as a central quantum system which coupled to a bosonic bath and compared with the result of the numerically exact method, namely the quasi-adiabatic path-integral (QUAPI) propagator technique. Good agreement is achieve between these two methods. And we find that it is possible for the reduction of decoherence with increasing temperature or with increasing TL-bath coupling, which verifies the previous findings.

The model is given as ( $\hbar = 1$ ):  $H = H_A + H_{AB} + H_B$  with

$$\begin{aligned} H_A &= \frac{\Delta_A}{2} \sigma_z^A, & H_{AB} &= \frac{g_0}{2} \sigma_x^A \sigma_x^B, \\ H_{B+bath} &= \frac{\Delta_B}{2} \sigma_z^B + \sum_k \omega_k b_k^\dagger b_k + \frac{\sigma_x^B}{2} \sum_k g_k (b_k^\dagger + b_k), \end{aligned} \quad (1)$$

where TSSs are characterized by pseudospin-1/2 operators  $\sigma_z^A$  and  $\sigma_z^B$  as usual,  $b_k$  and  $b_k^\dagger$

are the annihilation and creation operators of the bath mode.  $g_0$  and  $g_k$  are the coupling constants. Here, the anisotropic coupling between TSS-A and TSS-B subject to the z direction, and the B-bath coupling also to the z direction. The bath is fully defined by the spectral density  $J(\omega) \equiv \sum_k g_k^2 \delta(\omega - \omega_k)$ . We will use the piezoelectric spectral density, which describes the decoherence of a double quantum dots (DQD) qubit manufactured with GaAs [20, 21],

$$J^{TL}(\omega) = \alpha \omega \left( 1 - \frac{\omega_d}{\omega} \sin \frac{\omega}{\omega_d} \right) e^{-\omega^2/2\omega_l^2}, \quad (2)$$

where  $\omega_d$  is related to the center to center distance, and  $\omega_l$  to the dot size. Typically,  $\omega_d \sim 0.01(ps)^{-1}$  and  $\omega_l \sim 1(ps)^{-1}$  [21]. In the limit of  $\omega_d \rightarrow 0$ , one can find that, Eq. (2) goes back to the widely used Ohmic spectrum [22, 23].

## II. UNITARY TRANSFORMATION

On the analogy with Ref. [24], we apply a unitary transformation to the Hamiltonian,  $H' = \exp(S)H \exp(-S)$ , with the generator  $S \equiv \sum_k \frac{g_k}{2\omega_k} \xi_k (b_k^\dagger - b_k) \sigma_x^B + i\theta_0 \sigma_y^A \sigma_x^B$ . Therefore,

$$H'_A = \frac{\sigma_z^A}{2} (\Delta_A \cos \theta_0 + g_0 \sin \theta_0) \quad (3)$$

$$H'_{AB} = \frac{1}{2} \sigma_x^A \sigma_x^B (g_0 \cos \theta_0 - \Delta_A \sin \theta_0) - \frac{1}{2} \eta \Delta_B \sin \theta_0 i \sigma_y^A i \sigma_y^B \quad (4)$$

$$H'^{(0)}_{B+bath} = \frac{\sigma_z^B}{2} \eta \Delta_B \cos \theta_0 + \sum_k \omega_k b_k^\dagger b_k + \sum_k \frac{g_k^2}{4\omega_k} (\xi_k^2 - 2\xi_k) \quad (5)$$

$$H'^{(1)}_{B+bath} = \frac{\sigma_x^B}{2} \sum_k g_k (1 - \xi_k) (b_k^\dagger + b_k) - \frac{\eta \Delta_B \cos \theta_0}{2} i \sigma_y^B X_1 \quad (6)$$

$$H'^{(2)}_{B+bath} = \frac{\Delta_B \cos \theta_0}{2} [\sigma_z^B (\cosh X_1 - \eta) - i \sigma_y^B (\sinh X_1 - \eta X_1)] \\ + \frac{\Delta_B \sin \theta_0}{2} i \sigma_y^A [\sigma_z^B \sinh X_1 - i \sigma_y^B (\cosh X_1 - \eta)], \quad (7)$$

where  $X_1 = \sum_k \frac{g_k}{\omega_k} \xi_k (b_k^\dagger - b_k)$  and  $\eta$  is the thermodynamic average of  $\cosh X_1$ ,

$$\eta = \exp \left[ - \sum_k \frac{g_k^2}{2\omega_k^2} \xi_k^2 \coth(\beta\omega_k/2) \right], \quad (8)$$

which insures  $H'^{(2)}_{B+bath}$  contains only the terms of two-boson and multi-boson non-diagonal transitions and its contribution to physical quantities is  $(g_k^2)^2$  and higher. Suppose the B-Bath coupling is not strong, the last term of the above Hamiltonian are discarded in the

following discussion. Now if we let

$$\Delta'_A = \Delta_A \cos \theta_0 + g_0 \sin \theta_0, \Delta'_B = \eta \Delta_B \cos \theta_0, \quad (9)$$

$$g'_0 = (g_0 \cos \theta_0 - \Delta_A \sin \theta_0) = \eta \Delta_B \sin \theta_0, \quad (10)$$

$$g'_k = g_k(1 - \xi_k) = \eta \Delta_B \cos \theta_0 \frac{g_k}{\omega_k} \xi_k, \quad (11)$$

then,

$$\tan \theta_0 = \frac{g_0}{\Delta_A + \eta \Delta_B}, \quad (12)$$

$$\xi_k = \frac{\omega_k}{\omega_k + \eta \Delta_B \cos \theta_0}. \quad (13)$$

and the Hamiltonian becomes

$$H'_{A,B(0)} = \frac{\Delta'_A}{2} \sigma_z^A + \frac{\Delta'_B}{2} \sigma_z^B, \quad H'_{bath(0)} = \sum_k \omega_k b_k^\dagger b_k \quad (14)$$

$$H'_{AB} = g'_0 (\sigma_+^A \sigma_-^B + \sigma_-^A \sigma_+^B), \quad H'_{B+bath(1)} = \sum_k g'_k (\sigma_+^B b_k + \sigma_-^B b_k^\dagger). \quad (15)$$

where we have omitted the constant and the second order terms.

It is easy to check that  $(H'_{AB} + H'_{B+bath(1)})|g_0\rangle = 0$ , where  $|g_0\rangle$  is the ground state of  $H'_{A,B(0)} + H'_{bath(0)}$ . Therefore, the ground state energy is  $E_g = -\frac{1}{2}\Delta'_A - \frac{1}{2}\Delta'_B - \sum_k \frac{g_k^2}{4\omega_k} \xi_k (2 - \xi_k)$ . Note that, the transformed Hamiltonian  $H' = H'_{A,B(0)} + H'_{bath(0)} + H'_{AB} + H'_{B+bath(1)}$  is of similar form of that of RWA, which enable us to treat the system bath coupling much easier, but  $\Delta_A$ ,  $\Delta_B$ ,  $g_0/2$  and  $g_k/2$  are replaced by  $\Delta'_A$ ,  $\Delta'_B$  and  $g'_0$  and  $g'_k$  due to the contributions of anti-rotating terms. The renormalized effective coupling become much smaller than the original coupling, which enable the perturbation treatment works better than the ordinary Born approximation directly from original Hamiltonian.

Now, we can diagonalize  $H'_{A,B(0)} + H'_{AB}$  by a unitary transformation  $T$ ,

$$T = \begin{bmatrix} 1 & 0 & 0 & 0 \\ 0 & \cos(\theta) & \sin(\theta) & 0 \\ 0 & \sin(\theta) & -\cos(\theta) & 0 \\ 0 & 0 & 0 & 1 \end{bmatrix}. \quad (16)$$

where  $\tan 2\theta = 2g'_0/(\Delta'_A - \Delta'_B)$ . Then the Hamiltonian becomes  $\tilde{H} = \tilde{H}_0 + \tilde{H}_1$ ,

$$\tilde{H}_0 = \sum_{i=0}^3 \varepsilon_i |i\rangle \langle i| + \sum_k \omega_k b_k^\dagger b_k \quad (17)$$

$$\tilde{H}_1 = \sum_k g'_k (\varrho_+ b_k + \varrho_- b_k^\dagger). \quad (18)$$

where,  $\varepsilon_3 = -\varepsilon_0 = \frac{E_p}{2} \equiv \frac{1}{2}(\Delta'_A + \Delta'_B)$ ,  $\varepsilon_2 = -\varepsilon_1 = \frac{E_m}{2} \equiv \sqrt{\frac{1}{4}(\Delta'_A - \Delta'_B)^2 + g_0'^2}$ ,  $\varrho_+ = \varrho_-^\dagger \equiv \cos\theta(|3\rangle\langle 2| - |1\rangle\langle 0|) + \sin\theta(|2\rangle\langle 0| + |3\rangle\langle 1|)$ .

### III. MASTER EQUATION METHOD

Now, we write out the master equation for this 4-level system by treating  $\tilde{H}_0$  as unperturbed part, and  $\tilde{H}_1$  as perturbation, the reduced master equation is[25, 26]:

$$\frac{\partial \tilde{\rho}(t)}{\partial t} = -i [\tilde{H}_e, \tilde{\rho}(t)] - \int_0^t dt' X(t, t'). \quad (19)$$

where  $\tilde{H}_e \equiv \sum_{i=0}^3 \varepsilon_i |i\rangle\langle i|$  and  $X(t, t')$  is

$$\begin{aligned} X(t, t') &\equiv \text{Tr}_{bath} \left[ \tilde{H}_1, e^{-i\tilde{H}_0 t} [\tilde{H}_1, \tilde{\rho}(t-t')] e^{i\tilde{H}_0 t} \right] \\ &= \sum_k g_k'^2 n_k e^{i\omega_k t} \left[ \varrho_- e^{-i\tilde{H}_e t} \varrho_+ \tilde{\rho}(t-t') e^{i\tilde{H}_e t} - e^{-i\tilde{H}_e t} \varrho_+ \tilde{\rho}(t-t') e^{i\tilde{H}_e t} \varrho_- \right] \\ &+ \sum_k g_k'^2 n_k e^{-i\omega_k t} \left[ e^{-i\tilde{H}_e t} \tilde{\rho}(t-t') \varrho_- e^{i\tilde{H}_e t} \varrho_+ - \varrho_+ e^{-i\tilde{H}_e t} \tilde{\rho}(t-t') \varrho_- e^{i\tilde{H}_e t} \right] \\ &+ \sum_k g_k'^2 (n_k + 1) e^{-i\omega_k t} \left[ \varrho_+ e^{-i\tilde{H}_e t} \varrho_- \tilde{\rho}(t-t') e^{i\tilde{H}_e t} - e^{-i\tilde{H}_e t} \varrho_- \tilde{\rho}(t-t') e^{i\tilde{H}_e t} \varrho_+ \right] \\ &+ \sum_k g_k'^2 (n_k + 1) e^{i\omega_k t} \left[ e^{-i\tilde{H}_e t} \tilde{\rho}(t-t') \varrho_+ e^{i\tilde{H}_e t} \varrho_- - \varrho_- e^{-i\tilde{H}_e t} \tilde{\rho}(t-t') \varrho_+ e^{i\tilde{H}_e t} \right]. \end{aligned}$$

The above master equation is a  $4 \times 4$  matrix equation. According to the Kronecker product property and technique to Lyapunov matrix equation in matrix theory, by expanding the matrix  $\rho(t)$  into vector  $\overline{vec}[\rho(t)]$  along row, the equation becomes,

$$\left\{ \frac{\partial}{\partial t} + i [\tilde{H}_e \otimes I_{4 \times 4} - I_{4 \times 4} \otimes \tilde{H}_e] \right\} \overline{vec}[\tilde{\rho}(t)] = - \sum_k g_k'^2 \int_0^t dt' F_k(t-t') \overline{vec}[\tilde{\rho}(t')],$$

with

$$\begin{aligned} F_k(t) &\equiv n_k e^{i\omega_k t} \left[ \left( \varrho_- e^{-i\tilde{H}_e t} \varrho_+ \right) \otimes \left( e^{i\tilde{H}_e t} \right)^T - \left( e^{-i\tilde{H}_e t} \varrho_+ \right) \otimes \left( e^{i\tilde{H}_e t} \varrho_- \right)^T \right] \\ &+ n_k e^{-i\omega_k t} \left[ e^{-i\tilde{H}_e t} \otimes \left( \varrho_- e^{i\tilde{H}_e t} \varrho_+ \right)^T - \left( \varrho_+ e^{-i\tilde{H}_e t} \right) \otimes \left( \varrho_- e^{i\tilde{H}_e t} \right)^T \right] \\ &+ (n_k + 1) e^{-i\omega_k t} \left[ \left( \varrho_+ e^{-i\tilde{H}_e t} \varrho_- \right) \otimes \left( e^{i\tilde{H}_e t} \right)^T - \left( e^{-i\tilde{H}_e t} \varrho_- \right) \otimes \left( e^{i\tilde{H}_e t} \varrho_+ \right)^T \right] \\ &+ (n_k + 1) e^{i\omega_k t} \left[ e^{-i\tilde{H}_e t} \otimes \left( \varrho_+ e^{i\tilde{H}_e t} \varrho_- \right)^T - \left( \varrho_- e^{-i\tilde{H}_e t} \right) \otimes \left( \varrho_+ e^{i\tilde{H}_e t} \right)^T \right]. \end{aligned} \quad (20)$$

In order to seek the non-Markovian effect of the non-linear bath, we solve the above equation by using Laplace transformation, rather than by replacing  $\tilde{\rho}(t')$  as  $\tilde{\rho}(t)$  which is the usual treatment in the literature known as the Markovian approximation. After the Laplace transformation and convolution theorem, the master equation of the system can be obtained as:

$$U(P)_{16 \times 16} \overline{vec} \left[ \overline{\tilde{\rho}(P)} \right] = \overline{vec} [\tilde{\rho}(0)] \quad (21)$$

with

$$U(P)_{16 \times 16} = P I_{16 \times 16} + i \left[ \tilde{H}_e \otimes I_{4 \times 4} - I_{4 \times 4} \otimes \tilde{H}_e \right] + \sum_k g_k'^2 \overline{F_k(P)}_{16 \times 16},$$

and  $\overline{F_k(P)}_{16 \times 16}$  is the Laplace transformation of  $F_k(t)_{16 \times 16}$ . The master equation (21) leads to following uncoupled equations:

$$\left[ P + iE_p + (2n_k + 1) (\sin^2 \theta B_{7+} + \sin^2 \theta B_{8+}) \right] \tilde{\rho}_{14}(P) = \tilde{\rho}_{14}(0) \quad (22)$$

$$\left[ P - iE_p + (2n_k + 1) (\sin^2 \theta B_{7-} + \sin^2 \theta B_{8-}) \right] \tilde{\rho}_{41}(P) = \tilde{\rho}_{41}(0) \quad (23)$$

$$A_{44} \cdot \left[ \tilde{\rho}_{12}(P) \ \tilde{\rho}_{13}(P) \ \tilde{\rho}_{24}(P) \ \tilde{\rho}_{34}(P) \right]^T = \left[ \tilde{\rho}_{12}(0) \ \tilde{\rho}_{13}(0) \ \tilde{\rho}_{24}(0) \ \tilde{\rho}_{34}(0) \right]^T \quad (24)$$

$$A'_{44} \cdot \left[ \tilde{\rho}_{21}(P) \ \tilde{\rho}_{31}(P) \ \tilde{\rho}_{42}(P) \ \tilde{\rho}_{43}(P) \right]^T = \left[ \tilde{\rho}_{21}(0) \ \tilde{\rho}_{31}(0) \ \tilde{\rho}_{42}(0) \ \tilde{\rho}_{43}(0) \right]^T \quad (25)$$

$$A_{66} \cdot \left[ \tilde{\rho}_{11}(P) \ \tilde{\rho}_{22}(P) \ \tilde{\rho}_{23}(P) \ \tilde{\rho}_{32}(P) \ \tilde{\rho}_{33}(P) \ \tilde{\rho}_{44}(P) \right]^T = \left[ \tilde{\rho}_{11}(0) \ \tilde{\rho}_{22}(0) \ \tilde{\rho}_{23}(0) \ \tilde{\rho}_{32}(0) \ \tilde{\rho}_{33}(0) \ \tilde{\rho}_{44}(0) \right]^T \quad (26)$$

with the explicit definition of  $B_{7\pm}$ ,  $B_{8\pm}$ ,  $A_{44}$ ,  $A'_{44}$  and  $A_{66}$  being defined in Appendix.

Before solving these equations, we first have a look at the initial condition and the physical quantities. In this work, the physical quantity under our concern is the population difference  $P(t) \equiv \langle \sigma_x^A \rangle(t) = \text{Tr} [\rho(t) \sigma_x^A \otimes I_{2 \times 2}]$ . It can be rewritten as,

$$P(t) \equiv \text{Tr} \left[ \tilde{\rho}(t) \widetilde{\sigma_x^A} \right] \quad (27)$$

where  $\widetilde{\sigma_x^A} \equiv T e^S \sigma_x^A e^{-S} T = T (\sigma_x^A \cos \theta_0 + \sigma_z^A \sigma_x^B \sin \theta_0) T$ , which is

$$\widetilde{\sigma_x^A} = \begin{bmatrix} 0 & \sin(\theta + \theta_0) & -\cos(\theta + \theta_0) & 0 \\ \sin(\theta + \theta_0) & 0 & 0 & \cos(\theta + \theta_0) \\ -\cos(\theta + \theta_0) & 0 & 0 & \sin(\theta + \theta_0) \\ 0 & \cos(\theta + \theta_0) & \sin(\theta + \theta_0) & 0 \end{bmatrix} \quad (28)$$

thus,

$$\begin{aligned} P(t) &= (\tilde{\rho}_{12} + \tilde{\rho}_{34} + \tilde{\rho}_{21} + \tilde{\rho}_{43}) \sin(\theta + \theta_0) + (\tilde{\rho}_{24} - \tilde{\rho}_{13} + \tilde{\rho}_{42} - \tilde{\rho}_{31}) \cos(\theta + \theta_0) \\ &= 2\text{Re}(\tilde{\rho}_{12} + \tilde{\rho}_{34}) \sin(\theta + \theta_0) + 2\text{Re}(\tilde{\rho}_{24} - \tilde{\rho}_{13}) \cos(\theta + \theta_0). \end{aligned} \quad (29)$$

where the time dependant  $\tilde{\rho}(t)$  is replace by  $\tilde{\rho}$  for simplicity. From the above expression, we can see only Eq. (24) is relevant to the dynamics of population difference. According to Eq. (24), we have

$$\tilde{\rho}_{12}(P) + \tilde{\rho}_{34}(P) = \frac{(P + d_3) [\tilde{\rho}_{12}(0) + \tilde{\rho}_{34}(0)] + f [\tilde{\rho}_{24}(0) - \tilde{\rho}_{13}(0)]}{(P + d_1)(P + d_3) - f^2} \quad (30)$$

$$\tilde{\rho}_{24}(P) - \tilde{\rho}_{13}(P) = \frac{(P + d_1) [\tilde{\rho}_{24}(0) - \tilde{\rho}_{13}(0)] + f [\tilde{\rho}_{12}(0) + \tilde{\rho}_{34}(0)]}{(P + d_1)(P + d_3) - f^2} \quad (31)$$

$$d_1 = i(E_p - E_m)/2 + \sum_k (2n_k + 1) \cos^2 \theta B_{1+} \quad (32)$$

$$d_3 = i(E_p + E_m)/2 + \sum_k (2n_k + 1) \sin^2 \theta B_{1+} \quad (33)$$

$$f = \sum_k (2n_k + 1) \cos(\theta) \sin(\theta) B_{1+} \quad (34)$$

Suppose the system is in the upper eigenstate of  $\sigma_x^A$  and  $\sigma_x^B$  at the initial time  $t=0$ , therefore, the initial condition is given by

$$\rho(0) = \frac{1}{2} \begin{bmatrix} 1 & 1 \\ 1 & 1 \end{bmatrix} \otimes \frac{1}{2} \begin{bmatrix} 1 & 1 \\ 1 & 1 \end{bmatrix} = \frac{1}{4} \begin{bmatrix} 1 & 1 & 1 & 1 \\ 1 & 1 & 1 & 1 \\ 1 & 1 & 1 & 1 \\ 1 & 1 & 1 & 1 \end{bmatrix} \quad (35)$$

therefore,  $\tilde{\rho}(0) \equiv \frac{1}{4} T e^S (I_{2 \times 2}^A + \sigma_x^A) (I_{2 \times 2}^B + \sigma_x^B) e^{-S} T = \frac{1}{4} T (I_{2 \times 2}^A + \sigma_x^A \cos \theta_0 + \sigma_z^A \sigma_x^B \sin \theta_0) (I_{2 \times 2}^B + \sigma_x^B) T$ , which is

$$\tilde{\rho}(0) = \frac{1}{4} \begin{bmatrix} 1 + \sin(\theta_0) & \cos(\theta) + \sin(\theta + \theta_0) & \sin(\theta) - \cos(\theta + \theta_0) & \cos(\theta_0) \\ \cos(\theta) + \sin(\theta + \theta_0) & 1 + \sin(2\theta + \theta_0) & -\cos(2\theta + \theta_0) & \cos(\theta + \theta_0) + \sin(\theta) \\ \sin(\theta) - \cos(\theta + \theta_0) & -\cos(2\theta + \theta_0) & 1 - \sin(2\theta + \theta_0) & \sin(\theta + \theta_0) - \cos(\theta) \\ \cos(\theta_0) & \cos(\theta + \theta_0) + \sin(\theta) & \sin(\theta + \theta_0) - \cos(\theta) & 1 - \sin(\theta_0) \end{bmatrix}$$

from which we have

$$\tilde{\rho}_{12}(0) + \tilde{\rho}_{34}(0) = \sin(\theta + \theta_0)/2 \quad (36)$$

$$\tilde{\rho}_{24}(0) - \tilde{\rho}_{13}(0) = \cos(\theta + \theta_0)/2 \quad (37)$$

Therefore, the population difference is

$$P(t) = \text{Re} \left[ \mathcal{L}^{-1} \frac{(P + d_3) \sin^2 \Theta + f \sin \Theta \cos \Theta}{(P + d_1)(P + d_3) - f^2} \right] + \text{Re} \left[ \mathcal{L}^{-1} \frac{(P + d_1) \cos^2 \Theta + f \sin \Theta \cos \Theta}{(P + d_1)(P + d_3) - f^2} \right]. \quad (38)$$

where,  $\mathcal{L}^{-1}$  is the Laplace inversion operator which corresponds to  $\frac{1}{2\pi i} \int_{\sigma-i\infty}^{\sigma+i\infty} dP e^{Pt}$ ,  $\Theta \equiv \theta + \theta_0$  and

$$d_1 = i(E_p - E_m)/2 + \cos^2 \theta G(P) \quad (39)$$

$$d_3 = i(E_p + E_m)/2 + \sin^2 \theta G(P) \quad (40)$$

$$f = \cos(\theta) \sin(\theta) G(P) \quad (41)$$

$$G(P) = \int_0^\infty d\omega' \frac{J'(\omega')}{P + i\omega'} \coth(\beta\omega'), \quad (42)$$

with

$$J'(\omega) = J(\omega) \left( \frac{\eta \Delta_B \cos \theta_0}{\omega + \eta \Delta_B \cos \theta_0} \right)^2 \quad (43)$$

Here we would like to summarize the approximations we have made. Two approximations are made: The first one is the omission of  $H'_2$ , which is a 4th order approximation to the B-bath coupling. The second one is the Born approximation for deriving the master equation (19), which is consistent with the first approximation. Therefore, our treatment is applicable in low temperature for  $\alpha \ll 1$  and  $g_0, T \ll \Delta_A, \Delta_B$ .

#### IV. QUASI-ADIABATIC PATH-INTEGRAL METHOD

The QUAPI method is a numerical scheme based on a exact methodology [27–30]. The starting point of QUAPI method is the generic system-bath Hamiltonian

$$H = H_0 + \sum_j \frac{P_j^2}{2m_j} + \frac{1}{2} m_j \omega_j^2 (Q_j - c_j s / m_j \omega_j^2)^2.$$

where,  $H_0$  is the Hamiltonian for the bare system,  $s$  is the system coordinate, and  $Q_j$  are harmonic bath coordinates which are linearly coupled to the system coordinate. The characteristics of the bath are captured in the spectral density function

$$J(\omega) = \frac{\pi}{2} \sum_j \frac{c_j^2}{m_j \omega_j} \delta(\omega - \omega_j). \quad (44)$$



The reduced density matrix of the system evolve as  $\rho(s'', s', t) = \text{Tr}_{bath} \langle s'' | e^{-iH_0 t} \rho(0) e^{iH_0 t} | s' \rangle$ . If the path integral representation is discretized by  $N$  time steps of length  $\Delta t = t/N$  and the initial density matrix is assumed to be  $\rho(0) = \rho_s(0) \rho_{bath}(0)$ , the reduced density matrix takes the form

$$\begin{aligned} \rho(s'', s', t) = & \sum_{s_{N-1}^+} \sum_{s_{N-1}^-} \cdots \sum_{s_1^+} \sum_{s_1^-} \sum_{s_0^+} \sum_{s_0^-} \langle s'' | e^{-iH_0 \Delta t} | s_{N-1}^+ \rangle \cdots \langle s_1^+ | e^{-iH_0 \Delta t} | s_0^+ \rangle \\ & \langle s_0^+ | \rho_s(0) | s_0^- \rangle \langle s_0^- | e^{iH_0 \Delta t} | s_1^- \rangle \cdots \langle s_{N-1}^- | e^{iH_0 \Delta t} | s' \rangle I(s_0^+, s_0^-, s_1^+, s_1^-, \dots, s_{N-1}^+, s_{N-1}^-, s'', s', \Delta t) \end{aligned} \quad (45)$$

where the discrete variable representation (DVR) is used, the symbol  $s_k^\pm$  ( $k = 0, \dots, N-1$ ) denotes the system coordinate at the time  $k\Delta t$  on the forward and backward discretized Feynman path.  $|s_k^\pm\rangle$  ( $k = 0, \dots, N-1$ ) are the eigenstates of the system coordinate operator  $s$ . If a symmetric splitting of the time-evolution operator is employed  $e^{-iH\Delta t} = e^{-iH_{env}\Delta t/2} e^{-iH_0\Delta t} e^{iH_{env}\Delta t/2}$  with  $H_{env} = H - H_0$ , the corresponding influence functional reads

$$\begin{aligned} & I(s_0^+, s_0^-, s_1^+, s_1^-, \dots, s_{N-1}^+, s_{N-1}^-, s'', s', \Delta t) \\ = & \text{Tr}_{bath} \left[ e^{-iH_{env}(s'')\Delta t/2} e^{-iH_{env}(s_{N-1}^+)\Delta t} \dots e^{-iH_{env}(s_0^+)\Delta t/2} \right. \\ & \left. \times \rho_{bath}(0) e^{iH_{env}(s_0^-)\Delta t/2} \dots e^{iH_{env}(s_{N-1}^-)\Delta t} e^{iH_{env}(s')\Delta t/2} \right], \end{aligned} \quad (46)$$

One can find that the equilibrium position of the bath mode is adiabatically displaced along the system coordinate. If  $H_0$  provides a reasonable zeroth-order approximation to the dynamics, the quasi-adiabatic propagator is accurate for fairly large time steps. That is the quasi-adiabatic partitioning is a good representation when the bath property is mainly adiabatic, where the bath can keep up with the motion the system quickly. And the discrete path is to take into account of the non-adiabatic effect. For most of case, the quasi-adiabatic partitioning is reasonable especially when the system bath coupling is not strong. Therefore, the QUAPI discretization permits fairly large time steps when the adiabatic bath dominates the system dynamics. If the bath is purely adiabatic, even no discretization is needed. In the continuous limit (that is for  $\Delta t \rightarrow 0, N \rightarrow \infty$ ) the influence functional has been calculated

by Feynman and Vernon

$$\begin{aligned}
I = \exp \Bigg\{ & -\frac{1}{\hbar} \int_0^t dt' \int_0^{t'} dt'' [s^+(t') - s^-(t')] \\
& \times [\alpha(t' - t'')s^+(t'') - \alpha^*(t' - t'')s^-(t'')] \\
& - \frac{i}{\hbar} \int_0^t dt' \sum_j \frac{c_j^2}{2m_j\omega_j^2} [s^+(t')^2 - s^-(t')^2] \Bigg\} \quad (47)
\end{aligned}$$

where  $\alpha(t)$  is the bath response function, which can be expressed in terms of the spectral density as

$$\alpha(t) = \frac{1}{\pi} \int_0^\infty d\omega J(\omega) \left[ \coth \left( \frac{\beta\omega_j\hbar}{2} \cos(\omega_j t) - i \sin(\omega_j t) \right) \right]. \quad (48)$$

The last term in Eq.(47) arises from the "counter-terms" which are grouped with the bath Hamiltonian in the quasi-adiabatic splitting of the propagator. With the quasi-adiabatic discretization of the path integral, the influence functional, Eq. 47, takes the form

$$I = \exp \left\{ -\frac{1}{\hbar} \sum_{k=0}^N \sum_{k'=0}^k [s_k^+ - s_k^-] [\eta_{kk'} s_{k'}^+ - \eta_{kk'}^* s_{k'}^-] \right\},$$

where  $s_N^+ = s''$  and  $s_N^- = s'$ . The coefficients  $\eta_{kk'}$  can be obtained by substituting the discretized path into the Feynman-Vernon expression Eq.(47), which is given in Ref. [28].

The QUAPI method is essentially a tensor multiplication scheme, which exploits the observation that for environments characterized by broad spectra the response function  $\alpha(t)$  decays within a finite time interval. From the expression of the Feynman and Vernon influence functional Eq. (45), one can see that  $\alpha(t)$  characterizes nonlocal interactions, which connects system coordinate  $s(t')$  with  $s(t'')$ . The path  $s^\pm(t')$  at time  $t'$  is connected to the all the paths  $s^\pm(t'')$  at earlier times, which makes the evaluation of Eq. (45) a hard task. However, for a bath with a broad spectral density, such as a power law distribution of the spectral density,  $\alpha(t)$  has the finite memory, the memory length typically extending over only a few time slices when the quasi-adiabatic propagator is used to discretize the path integral. After discarding the negligible "long-distance interaction" with  $t' - t'' > \Delta k_{\max} \Delta t$  (or  $k - k' > \Delta k_{\max}$ ), the resulting path integral can be evaluated iteratively by multiplication of a tensor of rank  $2\Delta k_{\max}$ . In other words, there exists an augmented reduced density tensor of rank  $\Delta k_{\max}$  that obeys Markovian dynamics. The details of the multiplication scheme is discussed to a great extent in the literature, here we only present the essential parameters and mention briefly how to adopt it to our specific problem [27–30]. Here we discuss briefly the parameters used in the QUAPI method:

(i) The first parameter time-step  $\Delta t$  used for the quasi-adiabatic splitting of the path-integral. The memory time of the non-Markovian steps used by QUAPI is  $\Delta k_{max} \Delta t$ . The stability of the iterative density matrix propagation ensures the choices of  $\Delta t$ , it should not be too big nor too small, since the non-adiabatic effect requires more splitting of the path integral, that is smaller  $\Delta t$ . Whereas, since the memory length  $\Delta k_{max} \Delta t$  is usually a fixed value for a particular bath, QUAPI method prefers larger  $\Delta t$ , and consequently smaller  $\Delta k_{max}$  in consideration of the numerical efficiency (note that the algorithm scales exponentially with  $\Delta k_{max}$ , also see the discussion of the second parameter  $\Delta k_{max}$ ). Therefore, we should choose appropriate  $\Delta t$  to take into account both the non-adiabatic effect which prefer smaller time splitting and the non-Markov effect which prefer long memory time, typically, we choose  $\Delta t$  around  $\frac{2\pi}{20\Delta_A}$ , that is to choose tens of fraction of the cycle time of the bare system dynamics.

(ii) The second parameter is the memory steps  $\Delta k_{max}$ . If  $\Delta k_{max} \leq 1$ , the dynamics is purely Markovian. If the non-locality extends over longer time, terms with  $\Delta k_{max} > 1$  have to be included to obtain accurate results. In order to acquire converge result, in the practical implementation of QUAPI, one usually need to choose  $\Delta k_{max}$  large enough so that the response function reduces to negligible value within the length of  $\Delta k_{max} \Delta t$ . However this is a hard task, Since augmented propagator tensor  $A^{(\Delta k_{max})}$  is a vector of dimension  $(M^2)^{\Delta k_{max}}$  ( $M$  is the system dimension which is four here), and the corresponding tensor propagator  $T^{(2\Delta k_{max})}$  is a matrix of dimension  $(M^2)^{2\Delta k_{max}}$ , the QUAPI scheme scales exponentially with the parameter  $\Delta k_{max}$ . Thus one can not proceed the QUAPI calculation with very large  $\Delta k_{max}$ , and usually  $\Delta k_{max}$  is chosen less than 5 for  $M = 4$ , and even smaller for larger  $M$ .

## V. RESULTS AND DISCUSSION

We report  $P(t)$  as a function of time in Fig. 1 to Fig. 4 for  $\Delta_A = \Delta_B = 0.1\omega_l$ ,  $g_0 = 0.1\Delta_A$  and  $\omega_d = 0.05\omega_l$ . The analytical results are depicted in solid lines, and QUAPI results of different  $\Delta k$ 's are scatters with different colors and shapes. In Fig. 1, where  $\alpha$  is larger than  $g_0/\Delta_A$  which is set to be  $\alpha = 0.3$ , it shows that the decoherence is reduced by increasing the bath temperature  $T$  as predicted in Ref. [19]. However, in Fig. 2, where  $\alpha = 0.01$ , the coherence is not meliorated but rather damaged with increasing  $T$ . Similarly, in Fig. 3, decoherence reduction with bath coupling when  $\alpha = 0.3$  is possible, whereas, in Fig. 4, there

is only decoherence enhancing where  $\alpha = 0.01$ .

One can see both analytical and numerical shows good agreement. When the coupling is small, e.g.  $\alpha = 0.01, 0.02$  and  $0.03$  in Fig. 2 and Fig. 4, the two methods show perfect agreement, all the QUAPI results converges to our TRWA results as  $\Delta k$  increases. When  $\alpha$  becomes larger, e.g.  $\alpha = 0.3, 0.4$  and  $0.5$ , discrepancy appears, we attribute this discrepancy to that the QUAPI is not converged completely. Since when  $\alpha$  becomes large the non-adiabatic boson contributes significantly, one need small  $\Delta t$  to take into account of the non-adiabatic bosons. Whereas, the memory length is almost the same, consequently, one can not converge within  $\Delta k = 3$  which is the upper limit of our computation resources (note the algorithm scales exponentially as  $\Delta k$ ). Finally, as a check of our analytical method, we report the strong qubit-TL coupling case, where  $g_0 = \Delta$ . One can see perfect agreement is achieved between the analytical and the numerical methods.

## VI. CONCLUSION

In conclusion, without making RWA and Markov approximation, the dynamics of a qubit coupled with a spin-boson bath is investigated. We proposed an unitary transformation to treat this problem. The results of our analytical method show good agreement with QUAPI, even when the qubit-TL coupling is as strong as the TL spacing. And checked the decoherence behavior with varying bath temperature  $T$  and TLF-bath coupling. The decoherence of TSS-A can be reduced increasing bath temperature  $T$  or with increasing TL-bath coupling  $\alpha$  only when the A-B coupling is smaller than B-bath coupling.

## VII. ACKNOWLEDGEMENT

Part of the work of P. Huang is done when he visit IMSS, KEK in Japan. We gratefully acknowledge the support by China Scholarship Council, by the National Natural Science Foundation of China (Grant No.10734020) and the National Basic Research Program of China (Grant No. 2011CB922202) and by the Next Generation Supercomputer Project, Nanoscience Program, MEXT, Japan.

## Appendix A: The matrix form and the matrix elements of $\overline{F_k(P)}_{16 \times 16}$ and $U(P)_{16 \times 16}$

From Eq. (20), the laplace transform of  $F_k(t)$  is of following form,

$$\begin{bmatrix}
 F_{1,1} & 0 & 0 & 0 & 0 & F_{1,6} & F_{1,7} & 0 & 0 & F_{1,10} & F_{1,11} & 0 & 0 & 0 & 0 & 0 \\
 0 & F_{2,2} & F_{2,3} & 0 & 0 & 0 & 0 & F_{2,8} & 0 & 0 & 0 & F_{2,12} & 0 & 0 & 0 & 0 \\
 0 & F_{3,2} & F_{3,3} & 0 & 0 & 0 & 0 & F_{3,8} & 0 & 0 & 0 & F_{3,12} & 0 & 0 & 0 & 0 \\
 0 & 0 & 0 & F_{4,4} & 0 & 0 & 0 & 0 & 0 & 0 & 0 & 0 & 0 & 0 & 0 & 0 \\
 0 & 0 & 0 & 0 & F_{5,5} & 0 & 0 & 0 & F_{5,9} & 0 & 0 & 0 & 0 & F_{5,14} & F_{5,15} & 0 \\
 F_{6,1} & 0 & 0 & 0 & 0 & F_{6,6} & F_{6,7} & 0 & 0 & F_{6,10} & 0 & 0 & 0 & 0 & 0 & F_{6,16} \\
 F_{7,1} & 0 & 0 & 0 & 0 & F_{7,6} & F_{7,7} & 0 & 0 & 0 & F_{7,11} & 0 & 0 & 0 & 0 & F_{7,16} \\
 0 & F_{8,2} & F_{8,3} & 0 & 0 & 0 & 0 & F_{8,8} & 0 & 0 & 0 & F_{8,12} & 0 & 0 & 0 & 0 \\
 0 & 0 & 0 & 0 & F_{9,5} & 0 & 0 & 0 & F_{9,9} & 0 & 0 & 0 & 0 & F_{9,14} & F_{9,15} & 0 \\
 F_{10,1} & 0 & 0 & 0 & 0 & F_{10,6} & 0 & 0 & 0 & F_{10,10} & F_{10,11} & 0 & 0 & 0 & 0 & F_{10,16} \\
 F_{11,1} & 0 & 0 & 0 & 0 & 0 & F_{11,7} & 0 & 0 & F_{11,10} & F_{11,11} & 0 & 0 & 0 & 0 & F_{11,16} \\
 0 & F_{12,2} & F_{12,3} & 0 & 0 & 0 & 0 & F_{12,8} & 0 & 0 & 0 & F_{12,12} & 0 & 0 & 0 & 0 \\
 0 & 0 & 0 & 0 & 0 & 0 & 0 & 0 & 0 & 0 & 0 & 0 & F_{13,13} & 0 & 0 & 0 \\
 0 & 0 & 0 & 0 & F_{14,5} & 0 & 0 & 0 & F_{14,9} & 0 & 0 & 0 & 0 & F_{14,14} & F_{14,15} & 0 \\
 0 & 0 & 0 & 0 & F_{15,5} & 0 & 0 & 0 & F_{15,9} & 0 & 0 & 0 & 0 & F_{15,14} & F_{15,15} & 0 \\
 0 & 0 & 0 & 0 & 0 & F_{16,6} & F_{16,7} & 0 & 0 & F_{16,10} & F_{16,11} & 0 & 0 & 0 & 0 & F_{16,16}
 \end{bmatrix} \quad (A1)$$

where  $F_k(P)_{i,j}$  are expressed as  $F_{i,j}$  for simplicity. In order to save space, we do not give the explicit expressions of  $F_{i,j}$  here. On the other hand,  $\left[ \tilde{H}_e \otimes I_{4 \times 4} - I_{4 \times 4} \otimes \tilde{H}_e \right]$  is just a diagonal matrix. Therefore, from the definition of  $U(P)_{16 \times 16}$ ,

$$U(P)_{16 \times 16} = P I_{16 \times 16} + i \left[ \tilde{H}_e \otimes I_{4 \times 4} - I_{4 \times 4} \otimes \tilde{H}_e \right] + \sum_k g_k^2 \overline{F_k(P)}_{16 \times 16}, \quad (A2)$$

we can get each element of  $U(P)_{16 \times 16}$  as,

$$\begin{cases} U_{m,n} = \sum_k g_k^2 F_k(P)_{m,n} & \text{when } m \neq n \\ U_{m,m} = P + i \left[ \tilde{H}_e \otimes I_{4 \times 4} - I_{4 \times 4} \otimes \tilde{H}_e \right]_{m,m} + \sum_k g_k^2 F_k(P)_{m,m} \end{cases}$$

With the particular form of  $U(P)_{16 \times 16}$  one can decouple the master equation Eq. (21) into equation sets with smaller dimension as shown in Eq. (22)-(26), which are explicitly expressed in the subsequent Appendix. The parameters  $B_{\pm}$ 's which will be used in the

master equation sets are defined as,

$$\begin{aligned}
B_{1\pm} &= \frac{1}{P \pm i\omega_k}, B_{2\pm} = \frac{1}{P \pm i(\omega_k - E_m)}, \\
B_{3\pm} &= \frac{1}{P \pm i(\omega_k + E_m)}, B_{4\pm} = \frac{1}{P \pm i(\omega_k - E_p)}, \\
B_{5\pm} &= \frac{1}{P \pm i(\omega_k - \frac{E_p + E_m}{2})}, B_{6\pm} = \frac{1}{P \pm i(\omega_k - \frac{E_p - E_m}{2})}, \\
B_{7\pm} &= \frac{1}{P \pm i(\omega_k + \frac{E_p - E_m}{2})}, B_{8\pm} = \frac{1}{P \pm i(\omega_k + \frac{E_p + E_m}{2})}
\end{aligned}$$

### Appendix B: Solve the $4 \times 4$ Master equation

The master equation for  $\rho_{12}$ ,  $\rho_{13}$ ,  $\rho_{24}$  and  $\rho_{34}$  is

$$A_{44} \cdot \begin{bmatrix} \rho_{12}(P) & \rho_{13}(P) & \rho_{24}(P) & \rho_{34}(P) \end{bmatrix}^T = \begin{bmatrix} \rho_{12}(0) & \rho_{13}(0) & \rho_{24}(0) & \rho_{34}(0) \end{bmatrix}^T \quad (\text{B1})$$

where  $A_{44}$  is defined as

$$\begin{bmatrix}
P + d_1 + n_k^{(1)} d_{2k} & -\sum_k \frac{e_{1k} + e_{2k}}{2} & -n_k e_{1k} & -n_k d_{2k} \\
-\sum_k \frac{e_{1k} + e_{2k}}{2} & P + d_3 + n_k^{(1)} d_{4k} & n_k d_{4k} & n_k e_{1k} \\
-n_k^{(1)} e_{1k} & n_k^{(1)} d_{4k} & P + d_3 + n_k d_{4k} & -\sum_k \frac{e_{1k} - e_{2k}}{2} \\
-n_k^{(1)} d_{2k} & n_k^{(1)} e_{1k} & -\sum_k \frac{e_{1k} - e_{2k}}{2} & P + d_1 + n_k d_{2k}
\end{bmatrix} \quad (\text{B2})$$

where double indexes  $k$  indicate a sum over  $k$ ,  $n_k^{(1)} \equiv n_k + 1$  and

$$d_1 = i(E_p - E_m)/2 + \sum_k g_k'^2 (2n_k + 1) \cos^2 \theta B_{1+} \quad (\text{B3})$$

$$d_3 = i(E_p + E_m)/2 + \sum_k g_k'^2 (2n_k + 1) \sin^2 \theta B_{1+} \quad (\text{B4})$$

$$d_{2k} = g_k'^2 \sin^2 \theta (B_{2+} + B_{4-}) \quad (\text{B5})$$

$$d_{4k} = g_k'^2 \cos^2 \theta (B_{3+} + B_{4-}) \quad (\text{B6})$$

$$e_{1k} = g_k'^2 \cos(\theta) \sin(\theta) (B_{4-} + B_{1+}) \quad (\text{B7})$$

$$e_{2k} = g_k'^2 (2n_k + 1) \cos(\theta) \sin(\theta) (B_{4-} - B_{1+}) \quad (\text{B8})$$

By solving the above  $4 \times 4$  linear algebra equation, we can get

$$\tilde{\rho}_{12}(P) + \tilde{\rho}_{34}(P) = \frac{(P + d_3) [\tilde{\rho}_{12}(0) + \tilde{\rho}_{34}(0)] + f [\tilde{\rho}_{24}(0) - \tilde{\rho}_{13}(0)]}{(P + d_1)(P + d_3) - f^2} \quad (\text{B9})$$

$$\tilde{\rho}_{24}(P) - \tilde{\rho}_{13}(P) = \frac{(P + d_1) [\tilde{\rho}_{24}(0) - \tilde{\rho}_{13}(0)] + f [\tilde{\rho}_{12}(0) + \tilde{\rho}_{34}(0)]}{(P + d_1)(P + d_3) - f^2} \quad (\text{B10})$$

$$f \equiv \sum_k [(2n_k + 1) e_{1k} - e_{2k}] / 2 = \sum_k g_k'^2 (2n_k + 1) \cos(\theta) \sin(\theta) B_{1+}$$

As for the other  $4 \times 4$  master equation, since  $\rho_{21}$ ,  $\rho_{31}$ ,  $\rho_{42}$  and  $\rho_{43}$  is just the complex conjugate of  $\rho_{12}$ ,  $\rho_{13}$ ,  $\rho_{24}$  and  $\rho_{34}$ , we do not need to solve them, and ,on the other hand,  $A'_{44}$  is the very similar to  $A_{44}$ , the only difference is that  $B_+$ 's are changed to  $B_-$ 's and vice versa.

### Appendix C: Solve the $6 \times 6$ Master equation

The master equation for  $\rho_{11}$ ,  $\rho_{22}$ ,  $\rho_{23}$ ,  $\rho_{32}$ ,  $\rho_{33}$  and  $\rho_{44}$  is

$$A_{66} \cdot \begin{bmatrix} \tilde{\rho}_{11}(P) & \tilde{\rho}_{22}(P) & \tilde{\rho}_{23}(P) & \tilde{\rho}_{32}(P) & \tilde{\rho}_{33}(P) & \tilde{\rho}_{44}(P) \end{bmatrix}^T = \begin{bmatrix} \tilde{\rho}_{11}(0) & \tilde{\rho}_{22}(0) & \tilde{\rho}_{23}(0) & \tilde{\rho}_{32}(0) & \tilde{\rho}_{33}(0) & \tilde{\rho}_{44}(0) \end{bmatrix}^T \quad (C1)$$

$A_{66}$  defined as

$$\begin{bmatrix} P + n_k^{(1)}(a_{1k} + a_{2k}) & -n_k a_{1k} & -n_k b_{1k} & -n_k b_{2k} & -n_k a_{2k} & 0 \\ -n_k^{(1)} a_{1k} & P + n_k a_{1k} + n_k^{(1)} a_{2k} & -\frac{b_1 + b_3}{2} & -\frac{b_2 + b_4}{2} & 0 & -n_k a_{2k} \\ -n_k^{(1)} b_{1k} & -\frac{b_1 + b_3}{2} & P + a_3 & 0 & -\frac{b_1 - b_3}{2} & n_k b_{1k} \\ -n_k^{(1)} b_{2k} & -\frac{b_2 + b_4}{2} & 0 & P + a_4 & -\frac{b_2 - b_4}{2} & n_k b_{2k} \\ -n_k^{(1)} a_{2k} & 0 & -\frac{b_1 - b_3}{2} & -\frac{b_2 - b_4}{2} & P + n_k^{(1)} a_{1k} + n_k a_{2k} & -n_k a_{1k} \\ 0 & -n_k^{(1)} a_{2k} & n_k^{(1)} b_{1k} & n_k^{(1)} b_{2k} & -n_k^{(1)} a_{1k} & P + n_k(a_{1k} + a_{2k}) \end{bmatrix} \quad (C2)$$

where  $b_1 = \sum_k b_{1k}$ ,  $b_2 = \sum_k b_{2k}$ ,  $b_3 = \sum_k b_{3k}$ ,  $b_4 = \sum_k b_{4k}$ ,

$$a_{1k} = g_k'^2 \cos^2 \theta (B_{6+} + B_{6-}) \quad (C3)$$

$$a_{2k} = g_k'^2 \sin^2 \theta (B_{5+} + B_{5-}) \quad (C4)$$

$$a_3 = iE_m + \sum_k g_k'^2 (2n_k + 1) (\cos^2 \theta B_{5-} + \sin^2 \theta B_{6+}) \quad (C5)$$

$$a_4 = -iE_m + \sum_k g_k'^2 (2n_k + 1) (\sin^2 \theta B_{6-} + \cos^2 \theta B_{5+}) \quad (C6)$$

$$b_{1k} = g_k'^2 \cos(\theta) \sin(\theta) (B_{5-} + B_{6+}) \quad (C7)$$

$$b_{2k} = g_k'^2 \cos(\theta) \sin(\theta) (B_{6-} + B_{5+}) \quad (C8)$$

$$b_{3k} = g_k'^2 (2n_k + 1) \cos(\theta) \sin(\theta) (B_{5-} - B_{6+}) \quad (C9)$$

$$b_{4k} = g_k'^2 (2n_k + 1) \cos(\theta) \sin(\theta) (B_{6-} - B_{5+}) \quad (C10)$$

The analytical solution of this equation set is still out of our capability, however, it is irrelevant to the quantities which we are interested in. If we add the first two and last two lines of the master equation, we can find

$$\tilde{\rho}_{11}(P) + \tilde{\rho}_{22}(P) + \tilde{\rho}_{33}(P) + \tilde{\rho}_{44}(P) = 1/P \quad (\text{C11})$$

which ensures the conservation of the trace of the reduced density operator  $\text{Tr}\rho = 1$ .

- 
- [1] Y. Nakamura, Y. A. Pashkin, and J. S. Tsai, *Nature* **398**, 786 (1999).
  - [2] I. Chiorescu, P. Bertet, K. Semba, Y. Nakamura, C. Harmans, and J. E. Mooij, *Nature* **431**, 159 (2004), URL <http://dx.doi.org/10.1038/nature02831>.
  - [3] J. Q. You and F. Nori, *Phys. Today* **58**, 42 (2005).
  - [4] G. S. Engel, T. R. Calhoun, E. L. Read, T. K. Ahn, T. Mancal, Y. C. Cheng, R. E. Blankenship, and G. R. Fleming, *Nature* **446**, 782 (2007), URL <http://dx.doi.org/10.1038/nature05678>.
  - [5] H. Lee, Y. C. Cheng, and G. R. Fleming, *Science* **316**, 1462 (2007), URL <http://dx.doi.org/10.1126/science.1142188>.
  - [6] E. Paladino, L. Faoro, G. Falci, and R. Fazio, *Phys. Rev. Lett.* **88**, 228304 (2002), URL <http://dx.doi.org/10.1103/PhysRevLett.88.228304>.
  - [7] R. W. Simmonds, K. M. Lang, D. A. Hite, S. Nam, D. P. Pappas, and J. M. Martinis, *Phys. Rev. Lett.* **93**, 077003 (2004), URL <http://dx.doi.org/10.1103/PhysRevLett.93.077003>.
  - [8] G. Falci, A. D'Arrigo, A. Mastellone, and E. Paladino, *Phys. Rev. Lett.* **94**, 167002 (2005), URL <http://dx.doi.org/10.1103/PhysRevLett.94.167002>.
  - [9] A. Shnirman, G. Schon, I. Martin, and Y. Makhlin, *Phys. Rev. Lett.* **94**, 127002 (2005), URL <http://dx.doi.org/10.1103/PhysRevLett.94.127002>.
  - [10] B. Abel and F. Marquardt, *Phys. Rev. B* **78**, 201302 (2008), URL <http://dx.doi.org/10.1103/PhysRevB.78.201302>.
  - [11] M. Neeley, M. Ansmann, R. C. Bialczak, M. Hofheinz, N. Katz, E. Lucero, A. O'Connell, H. Wang, A. N. Cleland, and J. M. Martinis, *Nat. Phys.* **4**, 523 (2008), URL <http://dx.doi.org/10.1038/nphys972>.



- [12] A. Lupaşcu, P. Bertet, E. F. C. Driessen, C. Harmans, and J. E. Mooij, Phys. Rev. B **80**, 172506 (2009), URL <http://dx.doi.org/10.1103/PhysRevB.80.172506>.
- [13] J. Lisenfeld, C. Muller, J. H. Cole, P. Bushev, A. Lukashenko, A. Shnirman, and A. V. Ustinov, Phys. Rev. B **81**, 100511 (2010), URL <http://dx.doi.org/10.1103/PhysRevB.81.100511>.
- [14] H. Gassmann, F. Marquardt, and C. Bruder, Phys. Rev. E **66**, 041111 (2002), URL <http://dx.doi.org/10.1103/PhysRevE.66.041111>.
- [15] H. Gassmann and C. Bruder, Phys. Rev. B **72**, 035102 (2005), URL <http://dx.doi.org/10.1103/PhysRevB.72.035102>.
- [16] E. Paladino, M. Sassetti, G. Falci, and U. Weiss, Chem. Phys. **322**, 98 (2006), URL <http://dx.doi.org/10.1016/j.chemphys.2005.08.065>.
- [17] E. Paladino, M. Sassetti, G. Falci, and U. Weiss, Phys. Rev. B **77**, 041303 (2008), URL <http://dx.doi.org/10.1103/PhysRevB.77.041303>.
- [18] N. P. Oxtoby, A. Rivas, S. F. Huelga, and R. Fazio, New J. Phys. **11**, 063028 (2009), URL <http://dx.doi.org/10.1088/1367-2630/11/6/063028>.
- [19] A. Montina and F. T. Arecchi, Phys. Rev. Lett. **100**, 120401 (2008), URL <http://dx.doi.org/10.1103/PhysRevLett.100.120401>.
- [20] T. Brandes and B. Kramer, Phys. Rev. Lett. **83**, 3021 (1999), URL <http://dx.doi.org/10.1103/PhysRevLett.83.3021>.
- [21] Z. J. Wu, K. D. Zhu, X. Z. Yuan, Y. W. Jiang, and H. Zheng, Phys. Rev. B **71**, 205323 (2005), URL <http://dx.doi.org/10.1103/PhysRevB.71.205323>.
- [22] A. J. Leggett, S. Chakravarty, A. T. Dorsey, M. P. A. Fisher, A. Garg, and W. Zwerger, Rev. Mod. Phys. **59**, 1 (1987), URL <http://dx.doi.org/10.1103/RevModPhys.59.1>.
- [23] U. Weiss, *Quantum Dissipative Systems* (World Scientific, Singapore, 1999), 2nd ed.
- [24] H. Zheng, Eur. Phys. J. B **38**, 559 (2004), URL <http://dx.doi.org/10.1140/epjb/e2004-00152-7>.
- [25] D. P. DiVincenzo and D. Loss, Phys. Rev. B **71**, 035318 (2005), URL <http://dx.doi.org/10.1103/PhysRevB.71.035318>.
- [26] G. Burkard, Phys. Rev. B **79**, 125317 (2009), URL <http://dx.doi.org/10.1103/PhysRevB.79.125317>.
- [27] D. E. Makarov and N. Makri, Chem. Phys. Lett. **221**, 482 (1994), URL [http://dx.doi.org/10.1016/0009-2614\(94\)00275-4](http://dx.doi.org/10.1016/0009-2614(94)00275-4).

- [28] N. Makri and D. E. Makarov, J. Chem. Phys. **102**, 4600 (1995), URL <http://dx.doi.org/10.1063/1.469508>.
- [29] N. Makri and D. E. Makarov, J. Chem. Phys. **102**, 4611 (1995), URL <http://dx.doi.org/10.1063/1.469509>.
- [30] M. Thorwart, E. Paladino, and M. Grifoni, Chem. Phys. **296**, 333 (2004), URL <http://dx.doi.org/10.1016/j.chemphys.2003.10.007>.

### Figures Captions

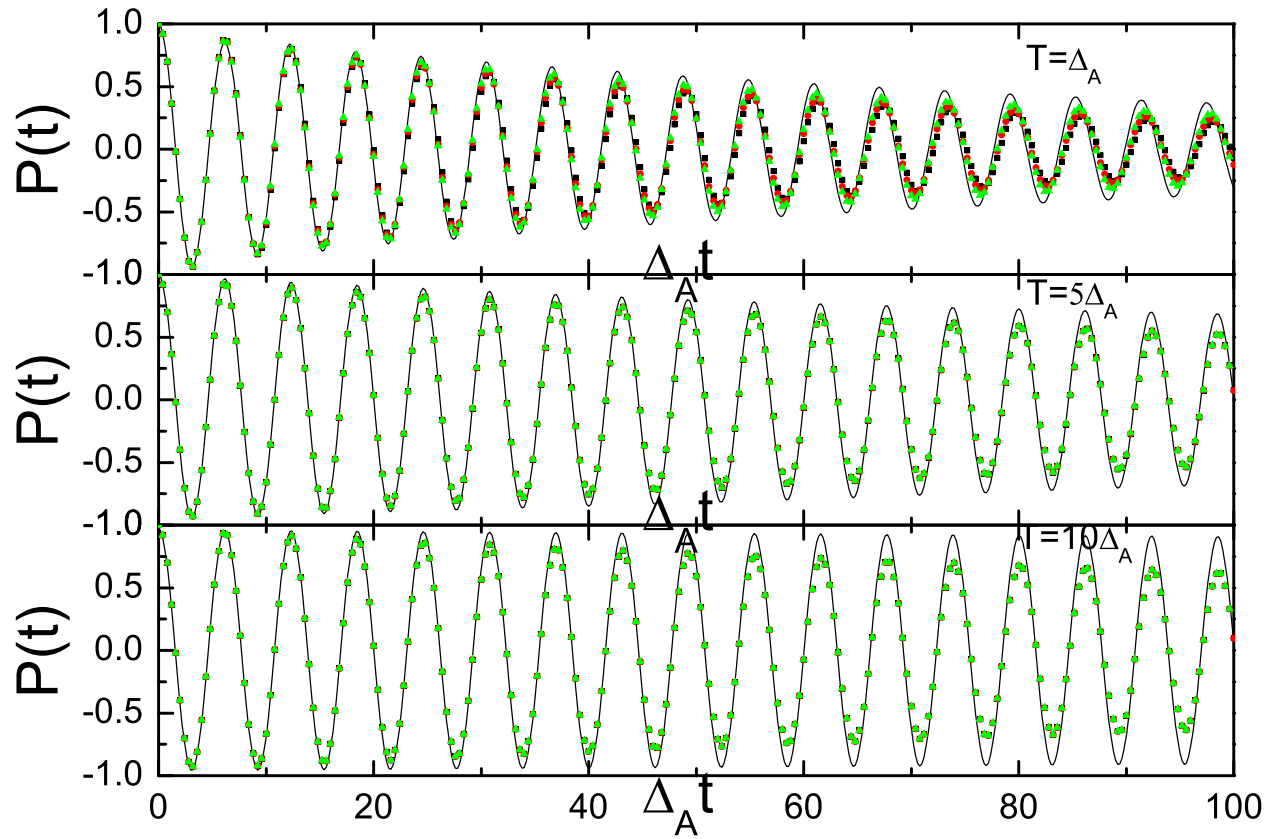
Fig. 1:  $P(t)$  is plotted as a function of time for different temperatures  $T/\Delta_A = 1, 5, 10$  with analytical method (solid lines) and the QUAPI methods with  $\Delta k = 1, 2$  and  $3$  (respectively black square, red circle and green triangle). The decoherence is reduced with temperature  $T$ . The parameters:  $\Delta_A = \Delta_B$ ,  $g_0 = 0.2\Delta_A$ ,  $\alpha = 0.3$ , and the QUAPI parameter  $\Delta t = 0.4/\Delta_A$ .

Fig. 2:  $P(t)$  is plotted as a function of time different temperatures  $T/\Delta_A = 0.1, 1, 5$  with analytical method (solid lines) and the QUAPI methods with  $\Delta k = 1, 2$  and  $3$  (respectively black square, red circle and green triangle). The decoherence is enhanced with  $T$ . Two frequencies are dominating the dynamics which agree with the results of Jaynes-Cummings model. The parameters:  $\Delta_A = \Delta_B$ ,  $g_0 = 0.2\Delta_A$ ,  $\alpha = 0.01$ , and the QUAPI parameter  $\Delta t = 0.4/\Delta_A$ .

Fig. 3:  $P(t)$  is plotted as a function of time for different TL-bath coupling  $\alpha = 0.3, 0.4$  and  $0.5$  with analytical method (solid lines) and the QUAPI methods with  $\Delta k = 1, 2$  and  $3$  (respectively black square, red circle and green triangle). The decoherence is reduced with temperature  $T$ . The parameters:  $\Delta_A = \Delta_B$ ,  $g_0 = 0.2\Delta_A$ ,  $T = 0.1\Delta_A$ , and the QUAPI parameter  $\Delta t = 0.4/\Delta_A$ .

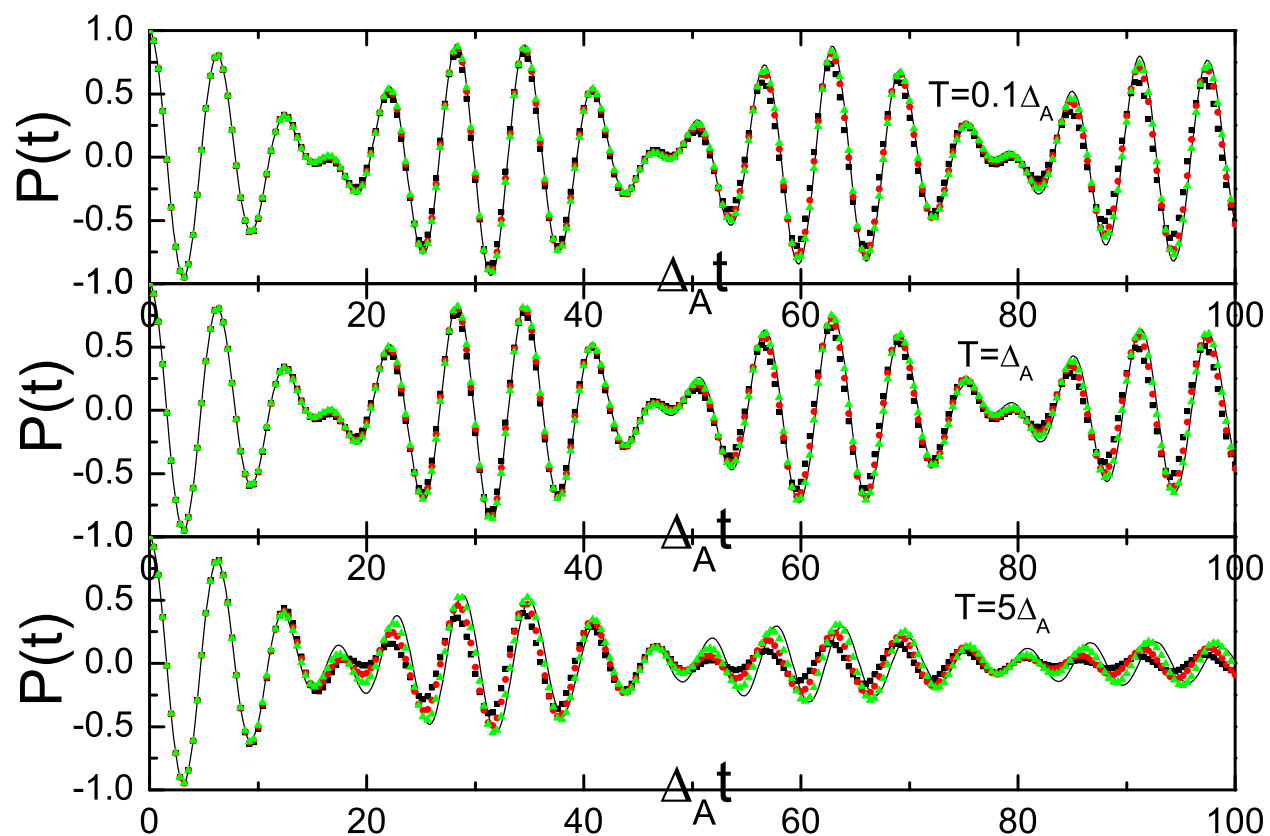
Fig. 4:  $P(t)$  is plotted as a function of time for different TL-bath coupling  $\alpha = 0.01, 0.02$  and  $0.03$  with analytical method (solid lines) and the QUAPI methods with  $\Delta k = 1, 2$  and  $3$  (respectively black square, red circle and green triangle). The decoherence is reduced with temperature  $T$ . The parameters:  $\Delta_A = \Delta_B$ ,  $g_0 = 0.2\Delta_A$ ,  $T = 0.1\Delta_A$ , and the QUAPI parameter  $\Delta t = 0.4/\Delta_A$ .

Fig. 5:  $P(t)$  is plotted as a function of time for strong qubit-TL coupling case  $g_0 = \Delta_A$  with analytical method (solid lines) and the QUAPI methods with  $\Delta k = 1, 2$  and  $3$  (respectively black square, red circle and green triangle). The parameters:  $\Delta_A = \Delta_B$ ,  $\alpha = 0.01$ , and the QUAPI parameter  $\Delta t = 0.4/\Delta_A$ .



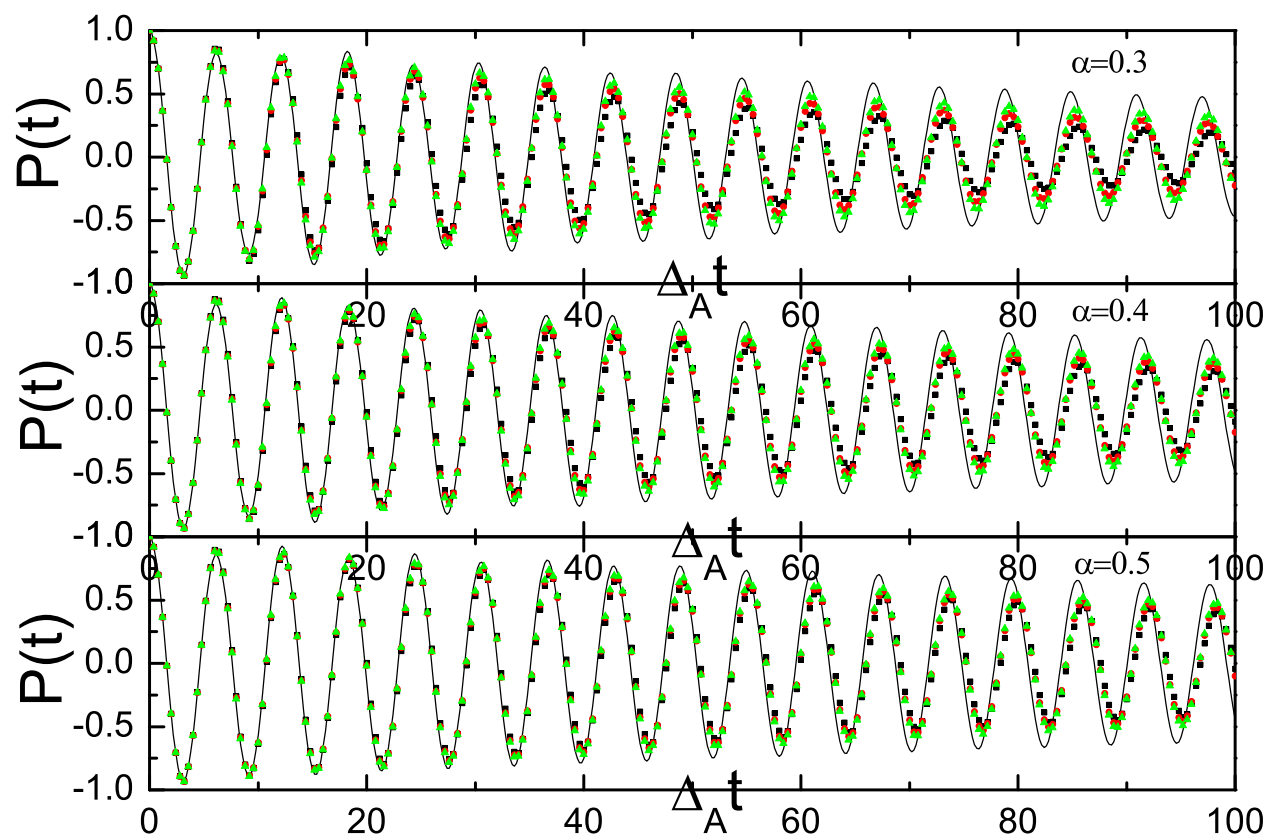
— TRWA  $\Delta_A = \Delta_B = 0.1\omega_l$   $g_0 = 0.2\Delta_A$   $\alpha = 0.3$   
quapi parameter:  $\Delta t = 0.4/\Delta_A$

- $\Delta k_{\max} = 1$
- $\Delta k_{\max} = 2$
- ▲  $\Delta k_{\max} = 3$



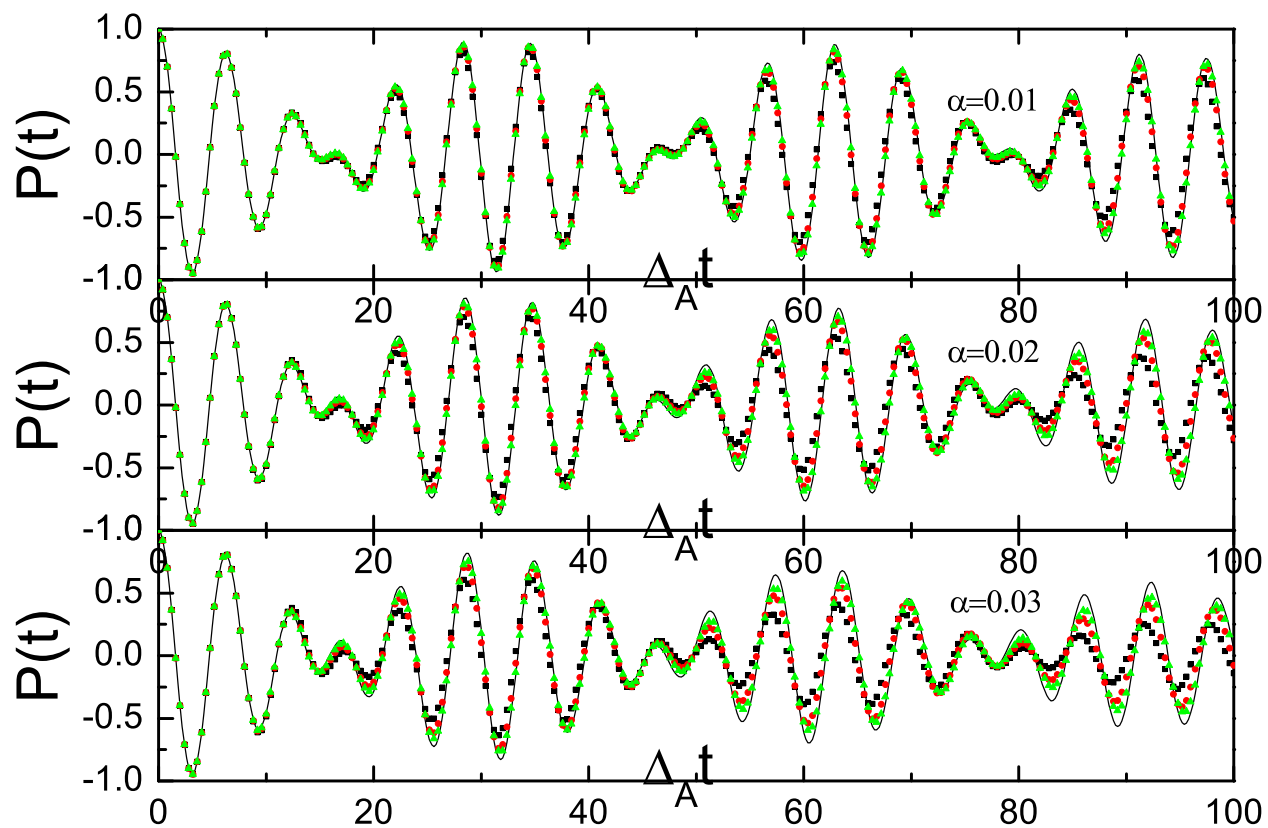
— TRWA  $\Delta_A=\Delta_B=0.1\omega_l$   $g_0=0.2\Delta_A$   $\alpha=0.01$   
 quapi parameter:  $\Delta t=0.4/\Delta_A$

- $\Delta k_{\max}=1$
- $\Delta k_{\max}=2$
- ▲  $\Delta k_{\max}=3$



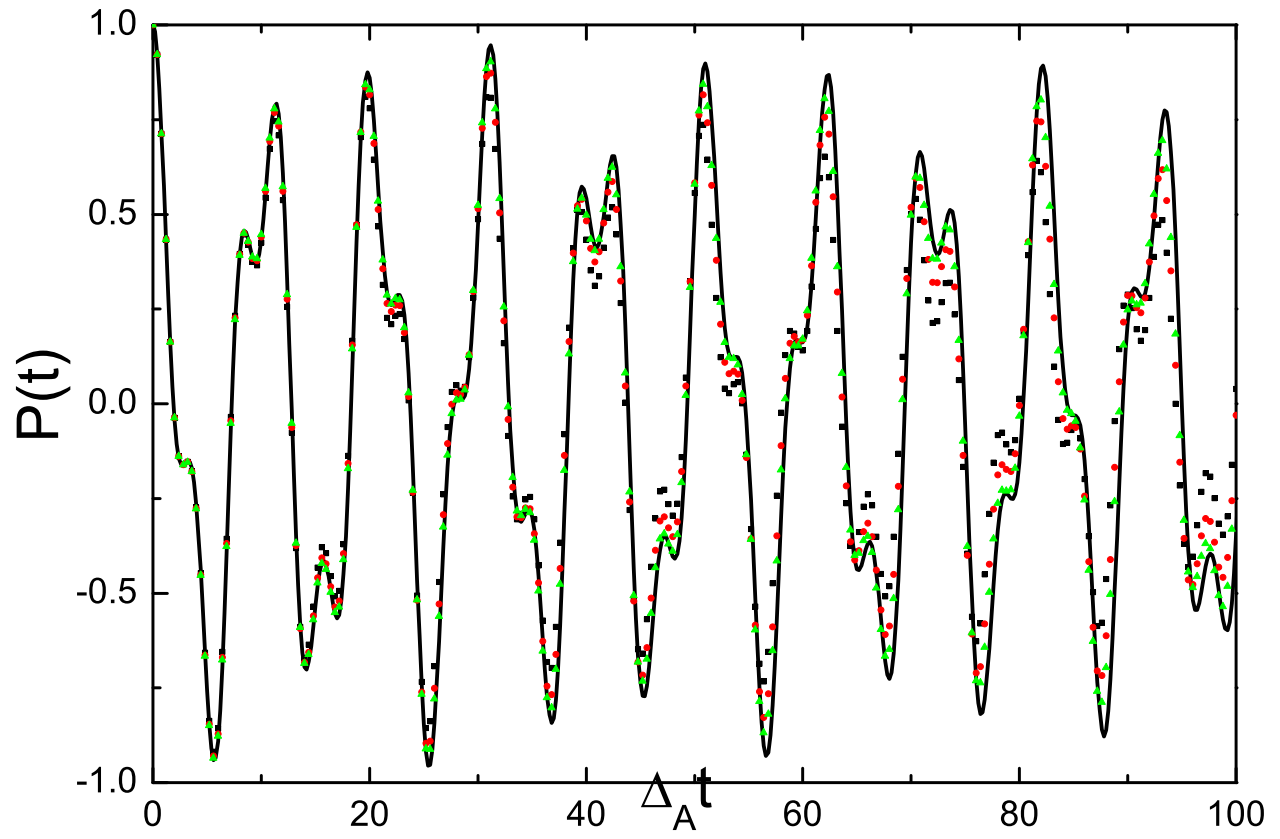
— TRWA  $\Delta_A = \Delta_B = 0.1 \omega_l$   $g_0 = 0.2 \Delta_A$   $T = 0.1 \Delta_A$   
 quapi parameter:  $\Delta t = 0.4 / \Delta_A$

- $\Delta k_{\max} = 1$
- $\Delta k_{\max} = 2$
- ▲  $\Delta k_{\max} = 3$



— TRWA  $\Delta_A = \Delta_B = 0.1 \omega_l$   $g_0 = 0.2 \Delta_A$   $T = 0.1 \Delta_A$   
 quapi parameter:  $\Delta t = 0.4 / \Delta_A$

- $\Delta k_{\max} = 1$
- $\Delta k_{\max} = 2$
- ▲  $\Delta k_{\max} = 3$



— TRWA  $\Delta_A = \Delta_B = 0.1 \omega_l$   $g_0 = \Delta_A$   $T = 0.1 \Delta_A$

quapi parameter:  $\Delta t = 0.4 / \Delta_A$

▪  $\Delta k_{\max} = 1$

•  $\Delta k_{\max} = 2$

▲  $\Delta k_{\max} = 3$